

EFFECT OF Sr-DOPING ON FERROELECTRIC AND DIELECTRIC PROPERTIES OF SOL-GEL SYNTHESIZED BaTiO₃ THIN FILMS

M. Y. SHAHID^a, A. ANWAR^b, F. MALIK^a, M. ASGHAR^a, M. F. WARSI^b,
S. Z. ILYAS^c

^a*Department of Physics, The Islamia University of Bahawalpur, Bahawalpur-63100, Pakistan*

^b*Department of Chemistry, The Islamia University of Bahawalpur, Bahawalpur-63100, Pakistan*

^c*Department of Physics, Allama Iqbal Open University, Islamabad, Pakistan*

Multicrystalline Sr-doped BaTiO₃ having the compositional formula BaTiO₃+ xSr (BTS), for x = 0.0, 0.025, 0.05, 0.1, 0.2, and 0.3 films have been obtained by sol-gel method. The films have been coated on Ti-substrates by means of spin – coating process. The effect of Sr-doping on the dielectric, ferroelectric and structural properties of the BTS films was studied by various characterization procedures. The X-ray diffraction (XRD) plots of BTS films show a slight shift in diffraction peaks to the higher 2-theta diffraction angle with the addition of Sr-content. Lattice parameters are calculated using XRD patterns and tetragonal phase structure has been confirmed. It is also observed that there is no phase change due to dopant incorporation. The XRD peaks become more sharp with increasing Sr-dopant concentration showing the improvement in crystallinity of the films. Scanning electron microscopy (SEM) of BTS films displays the crack free as well as uniform nature of the grown films. The EPMA data verified films compositions. The electrochemical measurements of BTS films display the variation of the current density (J) with the applied voltage (V). The polarization-voltage (P-V) measurements of these thin films annealed at 750 °C shows the reduction in the ferroelectric properties with addition of Sr-content. On the other hand dielectric constant –frequency (ϵ_r - f) measurements reveal that dielectric constant increases with Sr-dopant concentration. Among these BTS films, the compositions BaTiO₃+0.3Sr films have the maximum value of the dielectric constant 2.95041×10^{-35} measured at 10MHz frequency. The ferroelectric and dielectric properties of the sol-gel synthesized BTS thin films are influenced by the Sr-dopant concentration. The prominent effect of doping on both dielectric and ferroelectric properties of a material is highly appreciated for making high frequency devices.

(Received February 14, 2017; Accepted July 14, 2017)

Keywords: Sol-Gel, SEM, Barium Strontium Titanate (BST), Thin film, XRD, Dielectric and Ferroelectric properties

1. Introduction

Barium titanate is a famous dielectric material which is commonly used as an insulating layer in the fabrication of MIS structures. BaTiO₃ have many advantages over other frequently used dielectric materials and shows good properties such as high dielectric breakdown strength, maximum charge storage capacity, minimum leakage current density and good insulating property. It is also an attractive material for microwave devices because its dielectric constant can be varied by applying electric field externally. It has been demonstrated too that it works as an outstanding buffer layer in YBa₂Cu₃O_{7- δ} high-T_c superconductor grown on a variety of substrates, mainly on Al₂O₃ and Si [1, 2]. Because of wide band-gap, BaTiO₃ are transparent for the visible and infrared spectrum [3] and its electro-optic coefficients are very high that makes it an attractive candidate for active and passive optical components. In recent years, as-grown and doped BaTiO₃ thin films

have attracted much more attention as a result of their applications such as thermistors, pyroelectric detectors, multilayer hybrid capacitors and electro-optic devices. To date, many film growth processes such as pulsed laser deposition [4], chemical vapor deposition (CVD) [5], metal organic chemical vapor deposition [6-8], polymeric precursor method [9, 10], sol-gel synthesis [11] and molecular beam epitaxy (MBE) [5, 12] have been used to synthesize the BaTiO₃ thin films. Among these methods, the sol-gel process has gained much attention in the area of making thin films because it offers several advantages over the others such as better homogeneity, easier composition control, low equipment cost, low processing temperature and an easiest way to obtain good quality films [13, 14]. However, the film structure, dielectric and ferroelectric properties are strongly dependent on dopant type, its concentration and annealing temperature in addition to grain size and film thickness [15]. Sr-doped barium titanate having tetragonal (perovskite) structure is a common ferroelectric and high dielectric constant material. The ferroelectric and dielectric properties of BaTiO₃+ xSr greatly depend on the Sr-concentration. The fabrication of many novel devices is based on Sr-doped BaTiO₃ thin films that include thin film capacitors, phase shifters, optoelectronic devices, photovoltaic devices and humidity sensors [16]. Over the past few years because of the desired properties and applications, synthesis of Sr-doped BaTiO₃ thin film has gained much attention [17]. It is revealed from the detailed review of the literature that although some work on dielectric properties has been done to prepare thin films of Sr-doped BaTiO₃ using different growth techniques. No work is found in the literature about the fabrication of spin coated BTS thin films by sol-gel method using Ti-substrate. Hence the present article discusses the structure, dielectric and ferroelectric properties of Sr-doped BaTiO₃ thin films. For the present investigations, BaTiO₃ and Sr-doped BaTiO₃ thin films have been grown on Ti (100) substrates using sol-gel process.

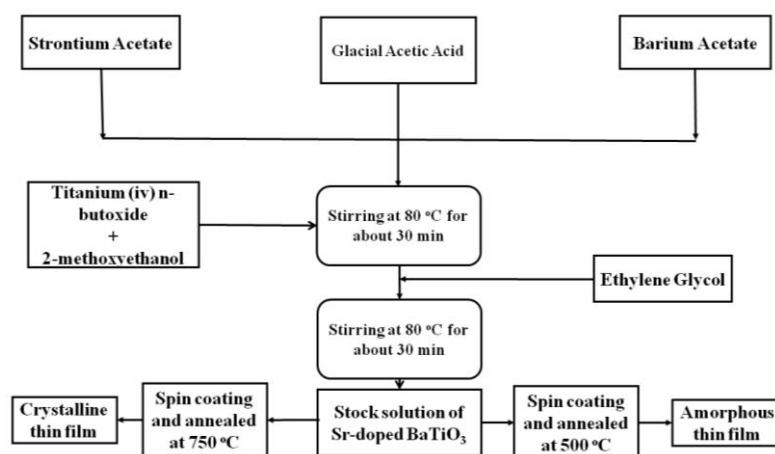
2. Experimental details

Sr-doped barium titanate thin films having the compositional formula BaTiO₃+ xSr (BTS), (here $x = 0.0, 0.025, 0.05, 0.1, 0.2, 0.3$ mol%) were prepared using sol-gel process. The preliminary materials used for these sample preparation were strontium acetate (Sr(C₂H₃O₂)₂·2H₂O) (Aldrich – 227,676, 99%), barium acetate (Ba(C₂H₃O₂)₂) (Aldrich, St. Louis, MO – 24,367, 99%) and titanium (iv) *n*-butoxide (C₁₆H₃₆O₄Ti) (Aldrich – 205,273, 97%). The materials were taken and weighted according to the stoichiometric amounts. First of all, the weighted amounts of strontium acetate and barium acetate were dissolved in heated glacial acetic acid. The solution was stirred until all the particles were dissolved and a clear solution was obtained. Secondly a stoichiometric amount of titanium (iv) *n*-butoxide was dissolved in 2-methoxyethanol and added to the first solution while keeping continuous stirring. In this solution, ethylene glycol was added in 1:3 proportions to the acetic acid to stabilize the solution. Different precursor solutions of BaTiO₃+ xSr having concentrations $x = 0.0, 0.025, 0.05, 0.1, 0.2,$ and 0.3 were prepared. The molarity of all solutions were kept 0.4 M for spin coating on titanium substrates. Before using the substrates, they were cleaned with acetone, isopropyl alcohol and de-ionized water at 80 °C for 10 minutes in each and then dried. The thin films were deposited on Ti-substrate (Titanium foils of 0.5 mm thickness) by spin coating process, each thin film consists of three layers of coating and each layer was subjected to a controlled heat treatment cycle in a rapid thermal processor. Every spin coated layer was dried at 100 °C for 10- min in the muffle furnace, in this way a thin film was made by three layers to get a required thickness of 380 nm. Finally, the whole film was annealed at 500 °C and 750 °C for 2-hour in air atmosphere. Table 1 gives the summary of the different amounts of compounds used for different compositions of BaTiO₃+ xSr samples preparation.

Table 1. Different amounts of compounds for various compositions of $\text{BaTiO}_3 + x\text{Sr}$.

Sr. No.	Sr-composition	X=0.3M	X=0.2M	X=0.1M	X=0.05M	X=0.025M	X=0.0M
1	Strontium acetate ($\text{Sr}(\text{C}_2\text{H}_3\text{O}_2)_2 \cdot 2\text{H}_2\text{O}$)	0.926g	0.617g	0.309g	0.154g	0.077g	0.0g
2	Titanium (iv) n-butoxide ($\text{Ti}(\text{C}_{16}\text{H}_{36}\text{O}_4)$)	2.11cm^3	2.11cm^3	2.11cm^3	2.11cm^3	2.11cm^3	2.11cm^3
3	Barium acetate ($\text{Ba}(\text{C}_2\text{H}_3\text{O}_2)_2$)	1.53g	1.53g	1.53g	1.53g	1.53g	1.53g
4	Ethylene glycol (dm^3)	5.0×10^{-3}					
5	Glacial acetic acid (dm^3)	1.5×10^{-2}					
6	2-methoxyethanol (dm^3)	1.5×10^{-2}					

The crystallization and phase formation of BTS films were analyzed using X-ray diffractometer (XRD) in a glancing angle mode using $\text{Cu-K}\alpha$ as a radiation source having wave length ($\lambda = 1.54056\text{\AA}$). The diffraction patterns of films were recorded by varying the diffraction angle (2θ) in the range $20\text{--}60^\circ$. The surface morphology of BTS films was studied by scanning electron microscope (SEM). Cross-sectional SEM micrographs were used to determine the film thickness. Electron microprobe analyzer (EPMA) was used to verify the elemental compositions at the different spots of BTS thin films. For electrical characterization, 200 nm gold thin film was deposited on the sample surface by thermal evaporation method to make a configuration like metal–dielectric–metal. The dielectric properties of Sr-doped BaTiO_3 thin films were measured using impedance/gain phase analyzer. Polarization–applied voltage hysteresis measurements were done using a modified Sawyer Tower circuit. AC electrochemical measurements were done with a Solartron 1260 frequency analyzer (FRA) in series with a Princeton Applied Research (PAR) 263A potentiostat. The schematic detailing shown in Figure 1 presents the summary of the procedure practically applied to prepare BTS thin films.

Figure 1. Schematic diagram representing key steps concerned in the preparation of Sr-doped BaTiO_3 films

3. Results and discussions

3.1 X-ray diffraction (XRD)

Figure 2 shows XRD graphs for the BTS thin films grown on Ti-substrate by sol-gel process annealed in air at 500°C and 750°C separately. It can be observed that all BTS thin films were amorphous in nature when annealing temperature was 500°C and on the other hand they

became polycrystalline when annealed at temperature of 750 °C [18]. The amorphous phase can be regarded as thermodynamically metastable state. Furthermore, the intensity of the (1 1 1) diffraction peak for all samples increased with annealing. It may be proposed that the crystallinity of the grown samples were improved by incorporation of Sr-atoms. The XRD results showed that the prepared samples have tetragonal phase [19, 20]. The calculated lattice parameters and hkl of selected peaks at different angle (2θ) for tetragonal structure were given in the Table 2 [21]. With the increase in Sr-concentration, the XRD lines shift towards larger 2θ angles showing lower values of lattice constant. The shifting of diffraction lines may be attributed due to the difference in size between the Sr^{2+} ions ($r = 0.113$ nm) and Ba^{2+} ions ($r = 0.135$ nm). This may be due to the decreased interatomic spacing of the small BTS nano-particles. The increased internal pressure in nano-particles results in an elastic, compressional volumetric strain and hence in a linear strain. This may sometimes lead to a reduced lattice parameters or inter-planar spacing [22, 23]. Moreover the intensity of all the XRD peaks increases with the addition of Sr-content and this effect is more clear from the plot of the sample in which Sr-concentration is $x=0.2$. From the above mentioned observations, it is resulted that addition of Sr-content to the BaTiO_3 enhances crystallization of these films.

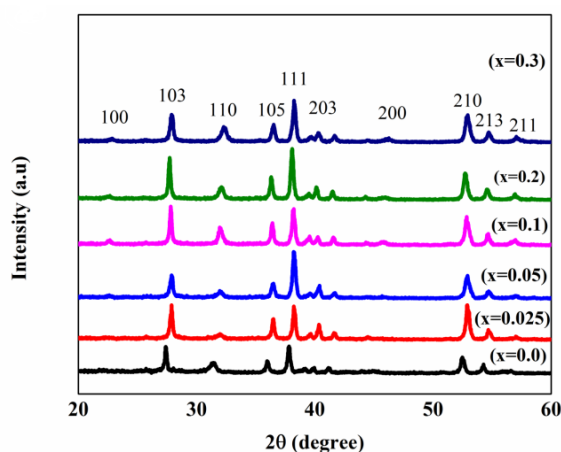


Figure 2. XRD spectra of sol-gel derived thin films of the compositions $\text{BaTiO}_3 + x\text{Sr}$ annealed at 750 °C in air atmosphere.

Table 2. The lattice constants, angle (2θ) and hkl of some selected peaks for tetragonal structure of $\text{BaTiO}_3 + x\text{Sr}$

Concentration	X= 0.3	X= 0.2	X= 0.1	X= 0.05	X= 0.025	X = 0.0	hkl
Angle 2θ (degree)	27.95	27.75	27.86	27.86	27.83	27.43	103
	32.32	32.15	32.06	32.03	32.06	31.35	110
	36.50	36.32	36.43	36.52	36.55	36.08	105
	38.24	38.09	38.27	38.27	38.24	37.83	111
	40.32	40.19	40.28	40.37	40.37	40.02	203
	52.93	52.78	52.84	52.96	52.96	52.49	210
	54.76	54.59	54.70	54.79	54.79	54.33	213
Lattice constant a (Å)	4.03	4.04	4.04	4.03	4.03	4.07	
Lattice constant c (Å)	16.83	16.95	16.85	16.81	16.80	17.03	
c (Å) / a (Å)	4.17	4.19	4.17	4.17	4.17	4.18	

3.2 Scanning electron microscope (SEM)

The SEM micrographs of the $\text{BaTiO}_3 + x\text{Sr}$ thin films ($x = 0, 0.025, 0.05, 0.1, 0.2,$ and 0.3) are shown in Figure 3. The SEM micrographs of doped BaTiO_3 reveal that the films are well crystallized and crack free in nature. The crystallinity of the BTS films is largely enhanced by the addition of Sr in the solutions. As can be observed in Figure 3, the surface cracks of $\text{BaTiO}_3 + x\text{Sr}$ thin films are dependent on Sr-concentration and the film cracks decrease with the increase in Sr-concentration [24]. Thin film made from a BaTiO_3 precursor solution with no Sr-content ($\text{BaTiO}_3 + x\text{Sr}$ for $x=0.0$) have a surface with large cracks shown in Figure 3 ($x=0.0$). On the other hand, BTS film made from a BaTiO_3 precursor solution with maximum Sr-dopant concentration ($\text{BaTiO}_3 + x\text{Sr}$ for $x=0.3$) in these samples, have a surface with no cracks (uniform) presented in Figure 3 ($x=0.3$). A similar pattern has been presented for MOD grown BST thin films with smaller grain sizes [25].

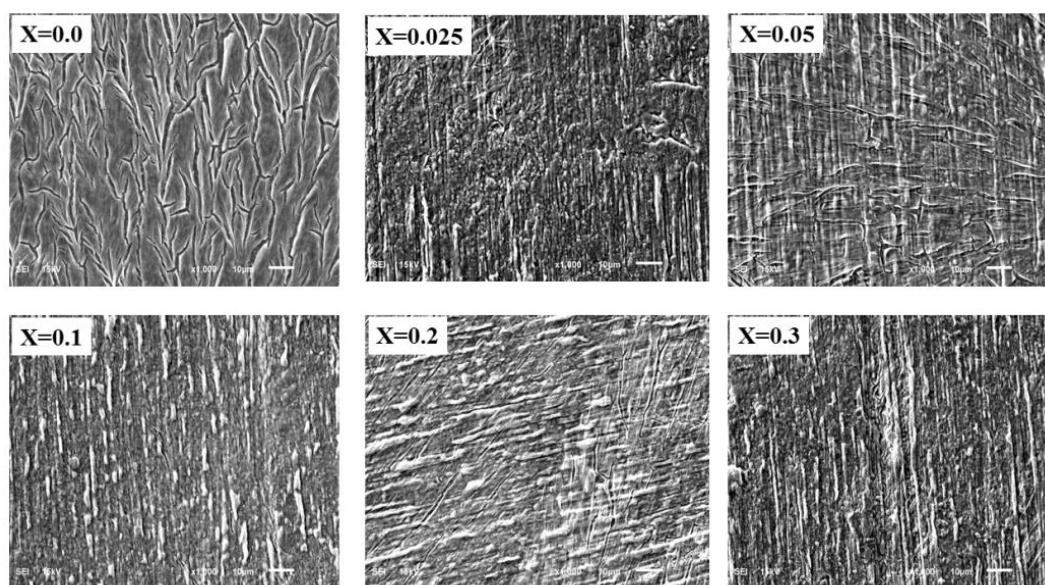


Figure 1. SEM micrographs of $\text{BaTiO}_3 + x\text{Sr}$ films with different Sr- concentration.

3.3 Electron probe micro analyzer (EPMA)

Table 3 shows the experimental results of the elemental compositional analysis of BTS thin films grown on Ti-substrate by sol-gel process. This method for elemental compositional analysis has certain advantages over other elemental compositional analysis methods especially when it comes to multicomponent metal oxides. EPMA data (Table 3) confirms the elemental composition of the samples and the samples were found to be of the same compositions that we have synthesized.

Table 3. EPMA data of the surface analysis of the composition $\text{BaTiO}_3 + x\text{Sr}$ thin films in molar percent

Composition	$\text{BaTiO}_3 + 0.3\text{Sr}$	$\text{BaTiO}_3 + 0.2\text{Sr}$	$\text{BaTiO}_3 + 0.1\text{Sr}$	$\text{BaTiO}_3 + 0.05\text{Sr}$	$\text{BaTiO}_3 + 0.025\text{Sr}$	BaTiO_3
Ba (%)	36.8726	40.6434	44.4380	47.3598	48.6484	49.1696
Ti (%)	36.8709	40.6446	44.4402	47.3628	48.6485	49.1699
Sr (%)	25.1532	17.5764	9.3074	4.8496	2.6702	-
Cl (%)	1.1033	1.1356	1.8145	0.4278	0.0329	1.6605

3.4 Ferroelectric properties

For electrical characterization measurements, a gold film of thickness 200 nm and area $(1.5 \times 1.5) \text{ cm}^2$ was deposited on the sample surface by thermal evaporating system to make a configuration such as metal-ferroelectric-metal (MFM). The room temperature polarization vs working voltage (P-V) hysteresis measurements of the composition $\text{BaTiO}_3 + x\text{Sr}$ (where $x = 0.0250, 0.050, 0.1, 0.2, 0.3$) are shown in the Figure 4. From these plots it is evident that the value of maximum polarization as well as the shape of the hysteresis loops mainly depends on Sr-dopant concentration. From the Figure 4, it is clear that the values of the remnant polarization of thin films decrease with increasing Sr-dopant concentration [23]. Majority of the films displayed the narrow ferroelectric hysteresis cycles, while a better defined loop was achieved from BaTiO_3 without Sr shown by Figure 4 ($x=0.0$). While the film made from a BaTiO_3 precursor solution with a maximum Sr ($\text{BaTiO}_3 + x\text{Sr}$ for $x=0.3$) in these samples showed a slim hysteresis P-V loop shown by Figure 4 ($x=0.3$). The ferroelectric properties of BTS thin films greatly depend on the Sr-concentration.

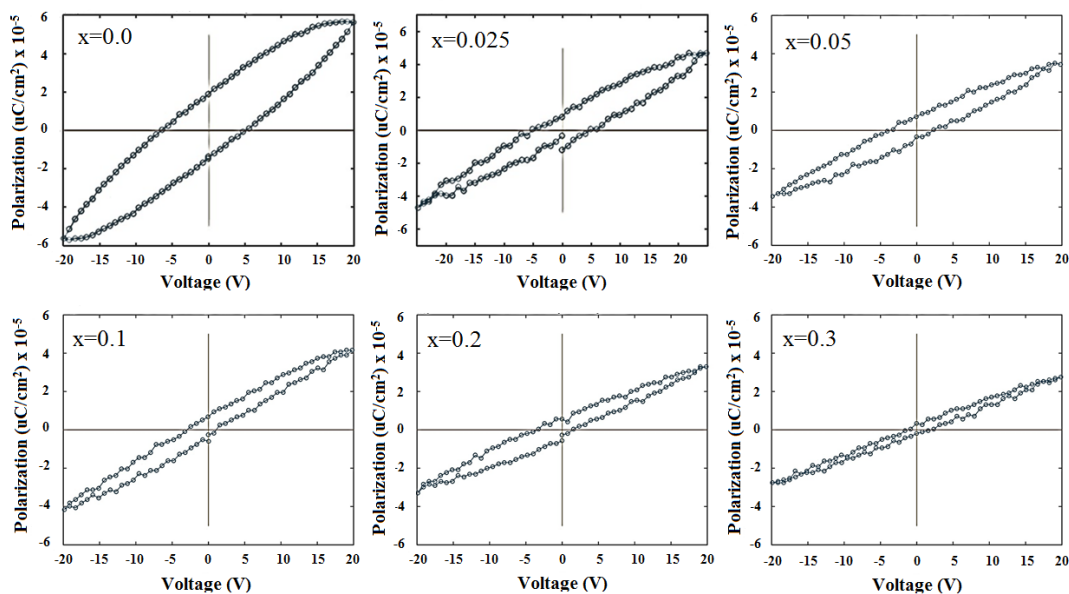


Figure 2: Polarization vs applied voltage (P-V) hysteresis measurements of un-doped and strontium-doped $\text{BaTiO}_3 + x\text{Sr}$ thin films (here $x = 0.0, 0.025, 0.05, 0.1, 0.2, \text{ and } 0.3$)

3.5 Electrochemical measurements

Current density-working potential (J - V) of BaTiO_3 thin films with different Sr-dopant concentrations are displayed in Figure 5. Increasing the voltage window much beyond +1000 mV to -1000 mV vs standard hydrogen electrode resulted in the evolution of hydrogen or oxygen. The broadening of the peaks observed in the films increases by increasing the Sr-content in $\text{BaTiO}_3 + x\text{Sr}$ thin films.

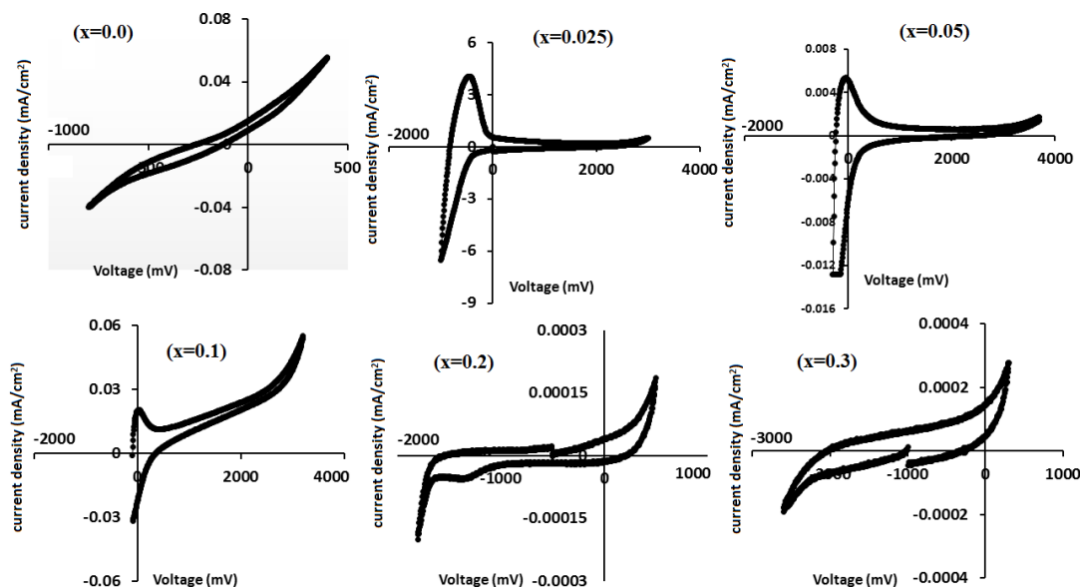


Figure 3. Typical voltammograms of $\text{BaTiO}_3 + x\text{Sr}$ thin films in $0.05\text{M H}_2\text{SO}_4$. 200mV/s scan rate was used

3.6 Dielectric properties

The materials for suitable device applications can be selected on the three parameters that are dielectric constant, dielectric loss and capacitance of the material. The dielectric constant (ϵ_r) of the given material is calculated using the formula.

$$\epsilon_r = \frac{Cd}{\epsilon_o A}$$

Where 'C' denotes the capacitance 'd' represents the thickness of the dielectric material (film), the Permittivity of free space is denoted by ' ϵ_o ' and 'A' show the area of the dielectric material (film). The variation of dielectric constant (ϵ_r) with operating frequency for the various compositions of the BTS thin films taken at room temperature is shown in Figure 6.

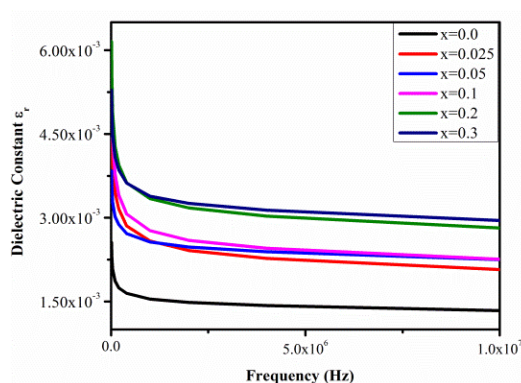


Figure 4. Dielectric permittivity vs applied frequency at room temperature of un-doped and strontium-doped $\text{BaTiO}_3 + x\text{Sr}$ thin films.

The thin film having composition $\text{BaTiO}_3 + 0.3\text{Sr}$ (maximum Sr-concentration) possesses the maximum dielectric constant in these samples. While the film made from a BaTiO_3 precursor solution having no Sr-content ($\text{BaTiO}_3 + x\text{Sr}$ for $x=0.0$) in these samples possesses the minimum dielectric constant in these samples. It is observed that ϵ_r increases with increasing Sr-dopant

concentration. A similar behavior has been presented for sol-gel derived BST thin films on Si-substrate[23, 26]. The dielectric constant decreases with increasing the operating frequency within the range of 10 KHz to 10 MHz but after 1MHz, the dielectric constants was only slightly decreased or almost remain constant showing that the grown BTS films have stable dielectric properties in the high frequency range. Table 4 shows the variation of dielectric constant with frequency of BTS thin films. Dielectric constant as a function of various Sr-concentrations of the samples is plotted and shown in the Figure 7. It is clear from this graph that the deviation of dielectric constant with composition of the samples is almost linear.

Table 4: Dielectric constant as a function of applied frequency data of un-doped and strontium-doped $BaTiO_3 + xSr$ thin films

Appl.Frequency (MHz)	0.01	0.02	0.10	0.40	2.00	10.00
X = 0.3	0.00529	0.00489	0.00409	0.00362	0.00326	0.00295
X = 0.2	0.00615	0.00549	0.00428	0.00363	0.00317	0.00282
X = 0.1	0.00606	0.0052	0.00378	0.00307	0.00259	0.00226
X = 0.05	0.00384	0.00355	0.00302	0.00272	0.00247	0.00225
X = 0.025	0.00513	0.0045	0.00345	0.00285	0.00241	0.00207
X = 0.0	0.00256	0.00229	0.00187	0.00165	0.00148	0.00134

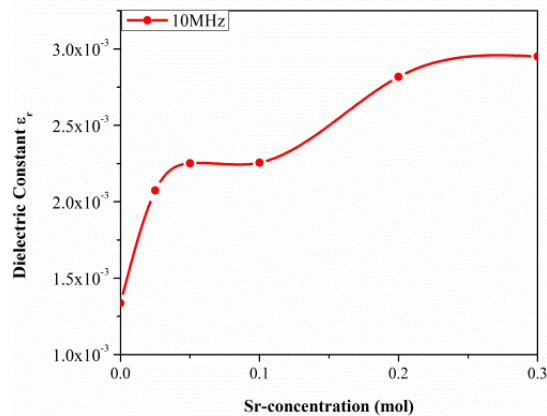


Figure 7. Variation in dielectric constant with Sr-content in $BaTiO_3$

4. Conclusions

Polycrystalline $BaTiO_3 + xSr$ thin films (here $x = 0, 0.025, 0.05, 0.1, 0.2,$ and 0.3) were grown on well cleaned Ti-substrate by low cost sol-gel process for the first time. XRD results showed that the films annealed at $750\text{ }^\circ\text{C}$ are polycrystalline nature and grown film has a tetragonal phase structure. The crystallinity of the film increases with increasing Sr-content. The diffraction peaks shift to the higher 2-theta angle with the addition of Sr-concentration.

The SEM micrographs displayed the homogeneous surface morphology and the EPMA results confirmed the composition of the grown thin films. The Dielectric constant increases with the Sr-incorporation while polarization decreases with Sr-concentration. On the basis of good characteristics and properties, such materials have high application in the manufacturing of advance technological devices.

Acknowledgements

Authors would like to pay their sincere thanks to Higher Education Commission (HEC) of Pakistan for financial support under the International Research Support Initiative Program (IRSIP) grant No. 1-8/HEC/HRD/2015/3728 and NRP (HEC / R&D / 2913), Center for Nanotechnology, University of Toronto, Toronto, Canada. The Islamia University of Bahawalpur, Pakistan, is also highly acknowledged.

References

- [1] S. Witanachchi, S. Patel, D. Shaw, H. Kwok, *Applied physics letters* **55**, 295 (1989).
- [2] J. Lee, Y. Bae, Y. Lee, *Semiconductor science and technology* **15**, 267 (2000).
- [3] A. Petraru, M. Siegert, M. Schmid, J. Schubert, C. Buchal, Cambridge Univ Press, 2001, pp. C8. 1.1.
- [4] T. García, P. Bartolo-Pérez, E. De Posada, J. Peña, M. Villagrán-Muniz, *Surface and Coatings Technology* **201**, 3621 (2006).
- [5] L. Wills, B.W. Wessels, D. Richeson, T.J. Marks, *Applied physics letters* **60**, 41 (1992).
- [6] T. Kim, Y. Yoon, S. Yom, C. Kim, *Applied surface science* **90**, 75 (1995).
- [7] Y. Yoon, W. Kang, H. Shin, S. Yom, T. Kim, J.Y. Lee, D. Choi, S.S. Baek, *Journal of applied physics* **73**, 1547 (1993).
- [8] B. Kwak, K. Zhang, E. Boyd, A. Erbil, B. Wilkens, *Journal of applied physics* **69**, 767 (1991).
- [9] S. Zanetti, E. Leite, E. Longo, J.A. Varela, *Journal of materials research* **13**, 2932 (1998).
- [10] S. Zanetti, E. Longo, J.A. Varela, E. Leite, *Materials Letters* **31**, 173 (1997).
- [11] C. Lemoine, B. Gilbert, B. Michaux, J.-P. Pirard, A. Lecloux, *Journal of non-crystalline solids* **175**, 1 (1994).
- [12] L. Beckers, J. Schubert, W. Zander, J. Ziesmann, A. Eckau, P. Leinenbach, C. Buchal, *Journal of applied physics* **83**, 3305 (1998).
- [13] M. Burgos, M. Langlet, *Thin Solid Films* **349**, 19 (1999).
- [14] M. Kamalasanan, N.D. Kumar, S. Chandra, *Journal of applied physics* **74**, 5679 (1993).
- [15] B. Block, B. Wessels, *Applied physics letters* **65**, 25 (1994).
- [16] S. Majumder, M. Jain, A. Martinez, R. Katiyar, F. Van Keuls, F. Miranda, *Journal of Applied Physics* **90**, 896 (2001).
- [17] S. Raja, C.S. Bellan, S. Sundaram, R. Rajamani, *Optik-International Journal for Light and Electron Optics* **127**, 3200 (2016).
- [18] T. Kineri, E. Matano, T. Tsuchiya, Preparation and optical properties of gold-dispersed BaTiO₃ thin films by sol-gel process, SPIE's 1994 International Symposium on Optics, Imaging, and Instrumentation, International Society for Optics and Photonics, 1994, pp. 145-150.
- [19] B.D. Begg, E.R. Vance, J. Nowotny, *Journal of the American Ceramic Society* **77**, 3186 (1994).
- [20] B. Stojanovic, A. Simoes, C. Paiva-Santos, C. Jovalekic, V. Mitic, J. A. Varela, *Journal of the European Ceramic Society* **25**, 1985 (2005).
- [21] P. Vitanov, A. Harizanova, T. Ivanova, D. Velkov, Z. Raytcheva, *Vacuum* **69**, 371 (2002).
- [22] V. Somani, S. J. Kalita, *Journal of electroceramics* **18**, 57 (2007).
- [23] R.W. Kelsall, I.W. Hamley, M. Geoghegan, *Nanoscale science and technology*, Wiley Online Library 2005.
- [24] S. Adikary, H. Chan, *Thin Solid Films*, **424**, 70 (2003).
- [25] M. S. Mohammed, R. Naik, J. V. Mantese, N. W. Schubring, A. L. Micheli, A. B. Catalan, *Journal of materials research* **11**, 2588 (1996).
- [26] S. Krupanidhi, C.-J. Peng, *Thin Solid Films* **305**, 144 (1997).